Galectin-3: a positive regulator of leukocyte recruitment in the inflamed microcirculation.1

Beatrice R. Gittens, **Jennifer V. Bodkin**, **Sussan Nourshargh**, **Mauro Perretti**, and **Dianne Cooper**

The William Harvey Research Institute, Barts and The London School of Medicine, Queen Mary University of London, London, United Kingdom

Abstract

In vivo and *ex vivo* imaging was used to investigate the function of galectin-3 (Gal-3) during the process of leukocyte recruitment to the inflamed microcirculation. The cremasteric microcirculation of wild-type (C57BL/6), Gal-3$^{-/-}$ and CX$_3$CR1$^{gfp/+}$ mice was assessed by intravital microscopy following PBS, IL-1β, TNF-α or recombinant Gal-3 treatment. These cellular responses were investigated further using flow-chamber assays, confocal microscopy, flow cytometry, PCR analysis and proteome array. We show that mechanisms mediating leukocyte slow rolling and emigration are impaired in Gal-3$^{-/-}$ mice, which could be due to impaired expression of cell adhesion molecules and an altered cell surface glycoproteome. Local (intrascrotal) administration of recombinant Gal-3 to wild-type mice resulted in a dose-dependent reduction in rolling velocity associated with increased numbers of adherent and emigrated leukocytes, approximately 50% of which were Ly6G-positive neutrophils. Intrascrotal administration of Gal-3 to CX$_3$CR1$^{gfp/+}$ mice confirmed that approximately equal numbers of monocytes are also recruited in response to this lectin. Exogenous Gal-3 treatment was accompanied by increased pro-inflammatory cytokines and chemokines within the local tissue. In conclusion, this study unveils novel biology for both exogenous and endogenous Gal-3 in promoting leukocyte recruitment during acute inflammation.

Introduction

Inflammation is a vital response to tissue injury or infection. Its effectiveness relies on the trafficking of leukocytes, predominantly neutrophils initially, to the site of injury. In acute inflammation this neutrophilic infiltrate is short-lived due to the co-ordinated release of pro-resolution mediators that terminate neutrophil recruitment and promote their efferocytosis leading to a return to homeostasis (1, 2). In chronic inflammation this resolution process fails and the leukocytic infiltrate becomes persistent, with, in the case of pathologies such as rheumatoid arthritis, repeated infiltration of neutrophils into the inflamed joint (3). Understanding the mechanisms by which leukocytes traffic from the bloodstream to the inflammatory site has been the focus of intense research over the past two decades and the

Author for correspondence: Dianne Cooper, William Harvey Research Institute, Barts and The London School of Medicine, Queen Mary University of London, Charterhouse Square, London EC1M 6BQ, United Kingdom. Phone: +442078825644; Fax: +442078826076; d.cooper@qmul.ac.uk.

leukocyte recruitment cascade is now a well-defined paradigm (4, 5). Although many of the adhesion molecules that drive this process have been identified, it is evident that leukocyte recruitment is multi-factorial and relies on the co-ordinated actions of many lipids and proteins including cytokines and chemokines, as well as the adhesion molecules themselves. Galectins, represent a family of proteins that have been ascribed pro-adhesive as well as chemotactic properties, however their role in neutrophil trafficking has not been systematically studied. Here we have focused on Galectin-3 (Gal-3), a molecule thought to have predominantly pro-inflammatory functions.

Galectins are a family of beta-galactoside binding proteins that elicit their effects by binding to exposed N-acetyllactosamine residues on cells (6). Specifically, Gal-3 binds glycoproteins that have been post-translationally modified by the glycosyltransferase Mgat5 (β1,6-N-acetylglucosaminyl transferase 5), which is responsible for the addition of β1,6 branched N-acetylglucosamine to the α-linked mannose of biantennary N-linked oligosaccharides (7). Since its characterization, Gal-3 has been implicated in a range of pathologies, many of which involve both acute and chronic inflammatory responses characterised by neutrophil infiltration. Levels of Gal-3 are increased during inflammation, both systemically and locally at the inflammatory site. In rheumatoid arthritis, Gal-3 localizes to sites of joint destruction in the synovium, with increased levels of the protein also found in sera and synovial fluids when compared to those from healthy controls or osteoarthritis patients (8). Circulating Gal-3 is also detectable in the sera of patients with Behcet's disease and heart failure with levels of this lectin in excess of 50ng/ml detectable (9, 10). In murine models of inflammation, elevated levels of Gal-3 in exudates has been found to correlate with increased neutrophil recruitment to the inflammatory site (11).

Due to its increased production during inflammation and the correlation between the presence of Gal-3 in inflammatory exudates and neutrophil infiltration we sought to determine whether Gal-3 directly modulates the leukocyte recruitment process undertaken by neutrophils as they traffic from the blood to the tissue. We have addressed the role of both the endogenous protein, through the use of Gal-3 null mice as well as the function of the recombinant protein. We have demonstrated for the first time that endogenous Gal-3 is specifically involved in leukocyte slow rolling and that the recombinant protein initiates recruitment of both neutrophils and monocytes to the cremaster microcirculation in an *in vivo* model of inflammation.

Materials and methods

Animals

Breeding founders for the Gal-3-/- mouse colony were obtained from the Consortium for Functional Glycomics on a C57BL/6 background and a colony was established at Charles River UK. Male mice bearing green fluorescent protein (GFP) under their CX3/CR1 promoter were kindly donated by Prof. S. Nourshargh at the Centre for Microvascular Research, QMUL, London. In all experiments age and sex-matched controls [wild type (WT) C57BL/6] were also purchased from Charles River UK. All animals were fed standard laboratory chow and water ad libitim and were housed in a 12h light-dark cycle under specific pathogen-free conditions. All experiments were performed with mice (20-28g),

strictly following UK Home Office regulations (Guidance on the Operation of Animals, Scientific Procedures Act, 1986).

Reagents

Recombinant mouse IL-1β and TNF-α and Power SYBR Green Mastermix were purchased from ThermoFisher Scientific (MA, USA). PE conjugated-anti-mouse Ly6g (Clone 1A8) and FITC-conjugated Ly-6G were purchased from BD Pharmingen. PE-conjugated Gal-3 (clone M3/83), PE-conjugated IgG2a isotype control (clone eBR2a), PE-conjugated CD11b (clone M1/70), APC-conjugated L-selectin (CD62L) (clone MEL-14), APC-conjugated IgG2a κ and PE-conjugated IgG2b k isotype controls, murine FC block and multi species 10x red blood cell lysis buffer were all purchased from eBiosciences (Hatfield, UK). Alexa Fluor® 488 Ly-6C (clone HK1.4) and pacific blue-conjugated Ly-6G (clone 1A8) were from Biolegend (Cambridge, UK). Streptavidin PE-conjugated secondary antibody was from Invitrogen (Paisley, UK). Alexa Fluor 488 conjugated fibrinogen was from Fisher Scientific (Loughborough, UK). Recombinant mouse E-selectin Fc Chimera, recombinant mouse ICAM-1 Fc Chimera and the mouse cytokine array panel A Proteome Profiler™ were from R&D Systems (Abingdon, UK). Alexa Fluor® 555 conjugated VE-Cadherin and Alexa Fluor® 647 conjugated MRP14 were kindly supplied by S.N.). Histopaque 1119 and 1077 was from Sigma Aldrich (Dorset, UK). Recombinant Gal-3 was kindly supplied by GalPharma Inc. (Japan). The following lectins were purchased from Vector Laboratories (Peterborough, UK): HPA, SNA, PNA, MAL II and Phaseolus vulgaris leucoagglutinin (L-PHA).

Intravital microscopy

Intravital microscopy of the cremaster muscle was carried out as previously described (12). Male mice were anaesthetised with Isofluorane gas before an intrascrotal (i.s.) injection of PBS (sham), IL-1β (30ng), TNF-α (300ng) or Gal-3 (200-1000ng) in a final volume of 400μl. The injection was carried out 2 or 4h before the vessel was recorded, allowing time for the 30min stabilization period after the surgery had been completed. Prior to the i.s. injection, some animals also underwent a tail-vein intravenous (i.v.) injection of fluorescent antibody, rat anti-mouse Ly-6G (2μg) in 200μL saline. Briefly, mice were anaesthetised using a mixture of xylazine (7.5 mg/kg; Rompun) and ketamine (150 mg/kg; Narketan) by intraperitoneal (i.p.) injection. The cremaster muscle was exteriorised and secured over the viewing stage; throughout the recordings it was superfused with bicarbonate buffered solution (BBS) held at 37°C. Brightfield recordings were carried out using a Zeiss Axioskop FS microscope (Carl Zeiss Ltd). Fluorescence microscopy was carried out using an Olympus BX61W1 microscope (Carl Zeiss Ltd.) connected to an Olympus BXUCB lamp, Uniblitz VCMD1 shutter driver and DG4-700 shutter instrument and recordings captured using Slidebook 5.0 software (Intelligent Imaging TTL). An Optical Doppler Velocimeter (Microvascular Research Institute, Texas A&M University) was used to ensure centerline red blood cell velocity remained adequate. Vessel segments of 100μm in post-capillary venules with a diameter of 20-40 μm, an adequate centerline velocity (500 s^{-1}) and no branches within 100μm either side of the segment to be analysed were chosen. Leukocyte rolling velocity (μm/s), adhesion (>30 s stationary) and emigration (50 μm by 100 μm either side of vessel) were quantified.

Ex vivo flow chamber assay

This assay was used to assess leukocyte behaviour under conditions of flow, which were generated using an automated syringe pump (Harvard Apparatus) connected to small-diameter tubing and chamber slides allowing observation of the leukocytes over a layer of recombinant E-Selectin. Ibidi µ-Slide VI0.4 cell microscopy chambers were coated with recombinant mouse E-selectin Fc Chimera (2µg/ml) in 100µL PBS/well for 2h at room temperature. The wells were blocked using 0.5% Tween-20 in PBS for 1h at room temperature. Murine whole blood was collected by cardiac puncture, diluted 1:10 in Hank's balanced salt solution (HBSS) and flowed through the chamber at 1.010ml/min for 3min. This was followed by HBSS at the same rate for 1min before image acquisition and subsequent offline analysis. In some experiments the whole blood was pre-treated for 15min at 37°C with recombinant Gal-3 (rGal-3; 10ng/ml) prior to flow. The flow chamber slides were viewed using a Nikon Eclipse TE3000 and 6 10s frames were collected for each well using a Q-Imaging Retiga EXi Digital Video Camera (Q-Imaging); recordings were analysed using Image Pro-Plus software (Media cybernetics).

In a further series of experiments crawling of bone marrow leukocytes on ICAM-1 was assessed. Cells were isolated from the tibias and femurs of mice as described previously (13). Briefly, bones were flushed with RPMI containing 10% FCS and 2mM EDTA and the resulting cell suspension was passed through a 100µm filter. Following hypotonic lysis of red blood cells with 0.2% NaCl, cells were washed in RPMI and resuspended in 1ml of ice-cold PBS. Cells were layered onto a double density gradient of histopaque and centrifuged for 30 min at 2,000 rpm without brake. Neutrophils were then collected from the interface between the 1119 and 1077 histopaque layers, counted and resuspended at 1×10^6/ml. Ibidi chamber slides were coated with recombinant mouse ICAM-1 Fc Chimera (2.5µg/ml). Bone marrow neutrophils were stimulated with TNFα (10ng/ml) and allowed to adhere within the chamber for 5 mins. HBSS was then flowed through the chamber at 2dyne/cm^2 and frames were recorded every 10 sec for 15 mins as described above. Cell crawling was analyzed using the cell-tracking function in ImageJ software, and tracks were analyzed utilizing Ibidi Chemotaxis and Migration Tool. Only cells that started and remained within the field of view over the entire course of video capture were analyzed. At least 45 cells were tracked per mouse.

Analysis of leukocyte glycosylation profile, cell adhesion molecule expression and integrin activation

Gal-3-/- or WT mice were deeply anaesthetised and up to 900µL of blood was collected by cardiac puncture into heparin-coated syringes (100µL of 100U/mL). Murine whole blood was treated for 15min at 37°C with PBS (Sham), murine IL-1β (1-100ng/ml) or murine TNF-α (10-200ng/ml) before centrifuging at 300 g for 5 min and aspiration of the supernatant. Cells were resuspended in murine FC Block (0.5µg/ml) and incubated for 10min on ice. The following rat anti-mouse primary antibodies were added directly to the wells and incubated for 45min on ice in the dark: PE-conjugated Gal-3 (8µg/ml), PE-conjugated IgG2a isotype control (8µg/ml), FITC-conjugated Ly-6G (5µg/ml), PE-conjugated CD11b (2µg/ml), PE-conjugated IgG2b k (2µg/ml), APC-conjugated L-selectin (1µg/ml), APC-conjugated IgG2a κ (1µg/ml), Alexa Fluor® 488 Ly-6C (2.5µg/ml). Red

blood cells were lysed with multi-species lysis buffer and the plate was washed twice in PBS-BSA before samples were transferred to flow cytometry tubes in 2% PFA and analysed on a FACSCalibur (BD Biosciences).

To assess CD11b activation, bone marrow neutrophils were stimulated with fMet-Leu-Phe (fMLP; 1μM) or Phorbol 12-myristate 13-acetate (PMA; 50ng/ml) for 15 mins in the presence of Alexa Fluor conjugated fibrinogen (250μg/ml). Neutrophils were subsequently labelled with pacific blue-conjugated Ly-6G (1.25μg/ml) and fibrinogen binding on the Ly-6G positive population was assessed on a BD LSRFortessa.

For the lectin binding assay, murine whole blood immediately underwent red cell lysis and following this were incubated with FC Block (0.5μg/mL) for 10 min before the addition of the following antibodies and biotinylated lectins for 45 min at room temperature: FITC-conjugated Ly-6G (5μg/ml), Alexa Fluor® 488 Ly-6C (2.5μg/ml), HPA (20μg/ml), SNA (166ng/ml), PNA (20μg/ml), MAL II (3.3μg/ml) and Phaseolus vulgaris leucoagglutinin (L-PHA; 4μg/ml; Vector Laboratories). The cells underwent incubation for 30 min at room temperature with a streptavidin PE-conjugated secondary antibody (120ng/ml in PBS-BSA) and fixation in 2% PFA before analysis on a FACSCalibur.

Isolation of murine lung endothelial cells

Murine lung endothelial cells (MLEC) were isolated from the lungs of Gal-3-/- or WT mice as described previously (14). Briefly, lungs were excised and placed in Ham's F12 media (Gibco) on ice. Following maceration, the tissue was further digested in 10mL 1mg/mL collagenase Type I-S for 2h at 37°C. The digest was diluted in 10mL MLEC media (equal parts low glucose DMEM and Ham's F12 (Gibco) containing heparin (100μg/mL; Sigma), penicillin (100U/mL), streptomycin (100μg/mL) and L-Glutamine (2mM; Sigma), endothelial cell growth supplement (25μg; AbD Serotech) and 20% FCS) and passed through a 19.5G needle followed by a 70μm cell-strainer (BD Falcon). The resulting cell suspension was cultured in flasks pre-coated with 10mL 0.1% Gelatin in PBS containing bovine collagen (30μg/mL, 97% Type I 3% type III; Nutacon) and bovine plasma fibronectin (10μg/mL; Sigma).

Endothelial cells were first purified by removal of contaminating macrophages using Dynabeads ((10μL/3mL); Dynal Biotech) and a rat anti-mouse CD16/32 (5μg/3mL; BD Biosciences) antibody. Sorted cells were then cultured until colonies of approximately 20 endothelial cells could be seen.

The culture was purified further by positive selection for the endothelial cells using ICAM-2/CD102 [Clone 3C4(mIC2/4); 10μg/3mL; BD Pharmingen]. 10mL MLEC media was used to resuspend the cells, which were then cultured until they reached 50% confluence, at which point the positive sort was repeated to enhance the culture.

Analysis of murine endothelial cell adhesion molecule expression

WT and Gal-3$^{-/-}$ MLEC were treated for 4 hours with PBS (sham) or murine IL-1β (1-100ng/mL) and then detached using Accutase. Cells were incubated with murine Fc Block (0.5μg/mL; eBiosciences). The following rat anti-mouse primary antibodies were

added directly to the cells with Fc Block and incubated on ice: PE-conjugated CD31 (clone MEC 13.3, 4μg/mL; BD Pharmingen), PE-conjugated CD54 (clone YN1/1.7.4, 2μg/mL; eBioscience), PE-conjugated IgG2bκ (2μg/mL; eBioscience), FITC-conjugated CD102 (clone 3C4, 10μg/mL; BD Pharmingen), purified CD62E (clone 10E9.6, 5μg/mL; BD Pharmingen). Cells were washed twice in PBS-BSA and transferred to flow cytometry tubes in 2% PFA before analysis on a FACSCalibur.

Ex vivo confocal microscopy of the cremaster

Cremasters from CX3/CR1 GFP mice were exteriorised and fixed in 4% PFA before permeabilisation and blocking in PBS containing 12.5% each of fetal bovine serum (FBS) and NGS and 0.5% Triton-X-100 for 2h at room temperature. Primary antibodies against VE-Cadherin (Alexa Fluor® 555 conjugated) and MRP14 (Alexa Fluor® 647 conjugated) were applied overnight at 4°C and the vessels were viewed using a Leica SP5 confocal microscope using a resonance scanner of 8000 Hz.

Assessment of murine cremaster mRNA

Murine cremaster muscles were dissected and snap frozen in LN_2 before tissue disruption using the Precellys 24 tissue homogeniser (5500 g, 3×20 s). The supernatant was further disrupted by passage through a 27G syringe before RNA isolation with the RNeasy kit and on-column DNase. RNA was reverse transcribed into cDNA. Quantitative real time PCR was performed using Power SYBR Green Mastermix (Applied Biosystems). Primers included those for Lgals3, Gapdh, Rpl32, Il-1b, tnf, Il-6, Ccl2, Cxcl1, Cxcl12, Ly-6G, Csf1r, Pecam1, Icam1 and Sele. Thermal cycling was carried out using the ABI Prism® 7900 Real Time PCR system according to manufacturer recommendations. The comparative Ct method (15) was used to measure gene transcription, where the Ct values were first normalised with an endogenous housekeeping gene and then to the control samples, which were used as a calibrator and given a value of 1 and the results were expressed as relative units based on $2^{-\Delta Ct}$.

Protein expression of cytokines and chemokines in the cremaster

Murine cremaster muscles were dissected and snap frozen in LN_2 before disruption in 600μL PBS containing protease inhibitors Aprotinin, Leupeptin and Pepstatin (all 10μg/ml) using the Precellys 24 tissue homogeniser (600 g, 2×30 s). The supernatant was collected and 1% Triton-X-100 was added before the samples underwent freezing at -80°C. After thawing the samples were centrifuged at 10,000 g for 5 min. A final protein quantity of 200 μg was then assessed using the mouse cytokine array panel A Proteome Profiler™ according to manufacturer instructions.

Statistical analysis

All data were analysed using GraphPad Prism 4 software. Data are expressed as mean ±standard error of the mean (SEM) of n experiments. All data were tested for normal distribution. Statistical significance was assessed using unpaired students t-tests, one-way analysis of variance (ANOVA) or two-way ANOVA with the appropriate post hoc test,

commonly Dunnett's post-test or the Tukey range test. In all cases a P value of 0.05 was considered significant.

Results

Endogenous Gal-3 is required for reduction in leukocyte rolling velocity in response to TNFα and IL-1β, and leukocyte emigration in response to IL-1β, in inflamed post-capillary venules

The cremasteric microcirculation of Gal-3^{-/-} mice was assessed after 4h treatment with TNFα (300ng) or IL-1β (30ng), reflecting the time taken to see significant changes in leukocyte recruitment in wild type mice (Fig. 1A-C). It is well established that these two stimuli are important pro-inflammatory modulators of the acute inflammatory response (16, 17) as well as in chronic pathologies, for example rheumatoid arthritis (18, 19). The administration of these cytokines *in vivo* results in leukocyte recruitment that may differ in mode; for example, an early study examining responses to both cytokines intradermally in the rabbit found that IL-1β-induced neutrophil extravasation peaked at 3-4h whereas TNFα-induced neutrophil extravasation was much quicker and also associated with protein synthesis-independent oedema formation (20). Following TNFα treatment, Gal-3^{-/-} mice displayed similar levels of leukocyte adhesion (Fig. 1B and D) and emigration (Fig. 1C and D); however, they lacked the reduction in rolling velocity observed in wild type animals that is characteristic of E-selectin-dependent rolling (Fig, 1A) (21). A similar observation was made in mice treated with IL-1β (30ng) where average rolling velocity was reduced in wild type mice but not in Gal-3^{-/-} animals (Fig. 1A). In addition, significantly fewer leukocytes emigrated in Gal-3^{-/-} mice after IL-1β treatment when compared to wild-type animals, a reduction that was not observed in response to TNFα (Fig. 1C).

Leukocyte binding to E-selectin and subsequent cellular morphological changes are disrupted in the absence of endogenous Gal-3

Since leukocyte rolling is dependent on selectin binding, with slow rolling predominantly mediated by E-selectin in this model (21), we next examined the role of Gal-3 in E-selectin-dependent rolling in greater depth. Experiments were performed under flow whereby whole blood from C57BL/6 or Gal-3^{-/-} mice was flown through chambers coated with recombinant E-selectin. We show that under conditions of flow, Gal-3^{-/-} leukocytes exhibit a reduced capacity to adhere to E-selectin when compared to wild type cells (Fig. 2A). Additionally, two types of leukocyte behaviours were observed; some cells remained phase bright, whereas some leukocytes displayed a more active phenotype and changed their morphology to become phase dark (Fig. 2C), likely due to E-selectin ligation, which initiates intracellular signalling pathways leading to neutrophil activation (22). We found that a smaller proportion (percentage of total cells) of Gal-3^{-/-} cells displayed phase dark morphology when compared to wild type cells (Fig. 2B). This phenotype was not rescued by the addition of plasma levels (10ng/ml, as assessed by ELISA) of rGal-3 to Gal-3^{-/-} blood (Fig. 2D). Importantly, there was no significant difference in white blood cell count (cells/μl) between wild type and Gal-3^{-/-} mice (WT 29.92±0.17 *vs.* KO 28.00±3.41, n.s); consequently, any differences observed can be attributed to changes in the leukocytes themselves. This is in line with full haematological reports published on the Consortium for Functional Genomics, which find

no differences in Gal-3$^{-/-}$ leukocyte cell counts when compared to wild type mice (23). These results suggest that in the absence of Gal-3, the cells lack the machinery needed to bind E-selectin and facilitate the downstream signalling pathways that are initiated once bound; thus, E-selectin ligands were studied in greater depth.

Murine neutrophils display reduced PNA and HPA lectin binding sites on their cell surface

Since there have been no reports of direct interactions between galectins and selectins, we hypothesised that lack of endogenous Gal-3 may affect the availability of selectin ligands. All selectin ligands carry sLe^x, commonly on α1,3-fucosylated and α2,3-sialylated O-glycans; though they are less well understood, E-selectin ligands specifically must be modified by a fucosyltransferase such as fucosyltransferase VII or IV to be functional. Hence the glycosylation pattern of Gal-3$^{-/-}$ leukocytes was assessed, as any inherent changes would greatly affect the ability of E-selectin ligands such as ESL-1, PSGL-1 and CD44 to bind. Since untreated Gal-3$^{-/-}$ leukocytes exhibited reduced capture to E-selectin under conditions of flow, basal levels of lectin binding by neutrophils was analysed by flow cytometry. This was carried out using cell markers and a panel of biotinylated lectins, which each bind glycans of different structures. When compared to their wild type counterparts, Gal-3$^{-/-}$ neutrophils were found to display comparable binding of the lectins SNA, L-PHA and MAL II but presented a marked reduction in binding of PNA and HPA (Fig. 3).

Cells lacking endogenous Gal-3 display altered ligand expression in response to IL-1 β and TNFα

We previously observed that endogenous Gal-3 is required for complete leukocyte emigration in response to IL-1β but not TNFα. These two classical stimuli are known to have differing and cell type-specific roles; IL-1β activates the endothelia directly whereas wild type neutrophils respond to TNFα by increasing their expression of β$_2$-integrin (CD18) and shedding L-selectin (24). We therefore assessed the effects of these two stimuli on adhesion molecule expression of wild type and Gal-3$^{-/-}$ leukocytes (Fig. 4).

Wild type or Gal-3$^{-/-}$ whole blood was treated for 10min at 37°C with vehicle (PBS), TNFα (50ng/mL) or IL-1β (50ng/mL) before cell staining with antibodies against CD11b and L-selectin as well as the neutrophil marker Ly-6G (Clone 1A8). In contrast to treatment with IL-1β, which did not alter expression from vehicle treated cell levels; treatment with TNFα increased neutrophil expression of CD11b in wild type cells (Fig. 4A). Furthermore, when compared to their wild type counterparts, Gal-3$^{-/-}$ neutrophils exhibited significantly reduced levels of CD11b basally and after cytokine treatment (Fig. 4A). To assess whether CD11b activation is also reduced in Gal-3-/- neutrophils, binding of Alexa488-conjugated fibrinogen to bone marrow-derived neutrophils from Gal-3-/- and wild type mice was measured. Stimulation of neutrophils with PMA (50ng/ml) significantly increased fibrinogen binding to both Gal-3-/- and wild-type neutrophils compared to untreated cells, however fibrinogen binding was not significantly different between the two genotypes (supplementary material Fig. S1A). In line with a lack of difference in CD11b activation between the two genotypes, there was no difference in neutrophil crawling (distance travelled or crawling velocity) on recombinant ICAM-1 between TNFα-stimulated bone marrow neutrophils from Gal-3-/- or wild type mice (supplementary material Fig. S1B and

C). In a similar fashion to CD11b expression patterns in wild type neutrophils, treatment with TNFα induced L-selectin shedding though IL-1β did not (Fig. 4C). However, L-selectin shedding was unaltered in the Gal-3^{-/-} neutrophils basally and after TNFα treatment (Fig. 4C).

In order to examine the direct effects of IL-1β on the endothelium, confluent wild type and Gal-3^{-/-} mEC were treated for 4h with the cytokine (1-100ng/ml). ICAM-1 and E-selectin expression levels were then quantified by flow cytometry. When compared to their wild type counterparts, Gal-3^{-/-} mEC expressed reduced E-selectin and ICAM-1 on their surface after IL-1β treatment (Fig. 4E, F).

Administration of exogenous Gal-3 results in neutrophil and monocyte recruitment to post-capillary venules

In addition to its intracellular localisation, Gal-3 is secreted and found extracellularly, where it exerts its effects predominantly by interacting with glycans on the cell surface and associated with the extracellular matrix. In order to establish whether exogenous Gal-3 is capable of initiating leukocyte recruitment to the cremasteric microcirculation in the absence of a classical inflammogen, a time-course using rGal-3 was carried out. Intravital microscopy was first performed using wild type C57BL/6 mice, which were injected i.s. with rGal-3 (500ng) 2 or 4h before subsequent analysis (Fig. 5). Leukocyte recruitment overall was increased at the 4h but not the 2h time-point with no significant differences observed between sham-treated animals and those treated with Gal-3 for 2h (Fig. 5A). In comparison, at 4h the microcirculation displayed significantly reduced leukocyte rolling velocities as well as significant increases in both adhesion and emigration (Fig. 5A). Once we had established that Gal-3 could elicit an inflammatory response, we were interested to establish whether the lectin would act dose-dependently and exhibit cell-type specific responses.

Following antibody validation, murine anti-Ly-6G was used to label neutrophils recruited to the cremaster in C57BL/6 mice treated with rGal-3 (200ng-1000ng in 400uL PBS i.s.). Rolling velocities were significantly reduced from sham levels in both 500ng and 1000ng-treated mice and this reduction was similar for Ly-6G -ve and Ly-6G +ve cells (Fig. 5B). Following 1000ng rGal-3 treatment, levels of both adherent and emigrated cells were significantly increased from sham for both Ly-6G -ve and Ly-6G +ve cells (Fig. 5B). This confirms that in this system exogenous Gal-3 can act specifically to increase neutrophil trafficking to the inflamed area *in vivo*, however, approximately half of the recruited cells remained unidentified. In order to investigate monocyte recruitment in isolation, the cremasteric microcirculation in $CX_3CR1^{gfp/+}$ mice was assessed 4h after intrascrotal injection of PBS (sham) or recombinant rGal-3 (1000ng). Monocyte rolling velocity was significantly reduced after rGal-3 treatment (Fig. 5D). This was in addition to increased adhesion and emigration of monocytes to the inflamed rGal-3-treated area (Fig. 5D). These results were confirmed using cremaster muscles from rGal-3-treated (1000ng) $CX_3CR1^{gfp/+}$ mice, which were exteriorised and stained using antibodies against VE-Cadherin and MRP14 (Fig. 5F). Similarly to the vessels analysed by intra-vital microscopy, mice treated with rGal-3 exhibited increased emigration of both neutrophils and monocytes when

compared to sham-treated animals and these cell types were present in the tissue in an approximate ratio of 50:50 (Fig. 5G).

Exogenous Gal-3 treatment results in increased pro-inflammatory cytokine and chemokine expression in the local tissue microenvironment

In order to further examine the effects of rGal-3 on the tissue after i.s. injection, real-time PCR analysis of expression of various inflammatory genes was carried out. The cremasters from C57BL/6 mice-treated i.s. with vehicle control (PBS) or rGal-3 (1000ng) were analysed. When compared to their sham-treated counterparts, cremaster muscle treated with rGal-3 displayed significantly increased mRNA for IL-1β, Keratinocyte-derived chemokine (KC), monocyte chemoattractant protein-1 (MCP-1) and IL-6 and there was a trend for increased TNFα (Fig. 6A). In contrast, the expression of SDF-1 was not changed in rGal-3-treated cremaster muscle when compared to sham preparations.

To confirm that this increase in pro-inflamatory gene expression results in increased protein, murine cremaster muscles were dissected following intrascrotal treatment for 4 hours rGal-3 (1000ng). Frozen cremasters were homogenised and a final protein quantity of 200μg was then assessed using the mouse cytokine array panel A Proteome Profiler™. The proteome array of rGal-3-treated cremaster samples displayed increased binding of many cytokines and chemokines, when compared to sham cremaster arrays (Fig. 6B). Cytokines increased after rGal-3 treatment included IFNγ, MCP-1, IL-6, KC, MIP-1α, MIP-2 (CXCL2) and TNFα. Crucially, these effects were not unidirectional and levels of some proteins in rGal-3-treated arrays were comparable or reduced when compared to control arrays, for example MIP-1β and BCA-1.

Administration of recombinant Gal-3 intravenously does not affect leukocyte recruitment or cell adhesion molecule expression

Despite treating locally with rGal-3, we wanted to ensure that the lectin was not entering the systemic circulation and acting on neutrophils and monocytes directly. Of note here are previous studies suggesting that Gal-3 may act as a soluble adhesion molecule for neutrophils *in vitro*, where it increased their binding to endothelial monolayers (11, 25). Additionally, Gal-3 promotes human neutrophil adherence to the extracellular matrix proteins laminin and fibronectin. This effect is dependent on the carbohydrate recognition domain and amino terminal of Gal-3 as well as being temperature and Ca^{2+}/Mg^{2+}-dependent, suggesting that Gal-3 oligomerizes at the cell surface (25). Furthermore, when the two cell types are incubated together *in vitro,* Gal-3 forms clusters between the endothelial cell surface and adherent neutrophils, these are concentrated at tricellular corners of the endothelium where these cells preferentially transmigrate (26). The cremasteric microcirculation was therefore assessed following intravenous administration of vehicle (saline, 200μL) or recombinant rGal-3 (150ng). It was found that administration of rGal-3 had no effect on leukocyte recruitment to the area over a 60 min period, suggesting that exogenous Gal-3 does not act on leukocytes or vascular endothelial cells directly, at least within 60 min (supplementary material Fig. S2A-D). Furthermore, analysis of leukocytes by flow cytometry following i.v. administration of rGal-3 revealed that the expression of CAMs such as PSGL-1, L-selectin, CD44 or CD11a, b and c was unchanged in response to this

lectin (supplementary material Fig. S2E). These results reflect those seen in the *ex vivo* flow chamber (Fig. 2D), where rGal-3 did not affect interactions of leukocytes with E-selectin in isolation.

Discussion

The goal of this study was to investigate whether Gal-3 acted as a positive regulator of leukocyte recruitment *in vivo*. The results reveal previously unreported roles for Gal-3 in controlling the dynamics of vascular leukocyte recruitment. We have shown that adhesion molecule expression is compromised in the absence of Gal-3 leading to reduced leukocyte trafficking *in vivo* and adhesion/activation *in vitro*. A pro-recruitment role for Gal-3 is further evidenced by the ability of the recombinant protein to induce the generation of multiple soluble pro-inflammatory mediators and to enhance leukocyte transmigration. Overall, these results suggest that Gal-3 is required for the efficient recruitment of leukocytes during an acute inflammatory response.

The actions of galectins are complex and depend on their cellular localisation with intracellular functions often at odds with their effects once released in the extracellular environment. This is the case for Gal-3, as the intracellular protein can inhibit T cell apoptosis (27), whilst extracellular Gal-3 induces apoptosis (28). It is also apparent that the actions of Gal-3 are stimulus specific, particularly when considering its role in neutrophil trafficking (29–31). Although previous studies suggest that Gal-3 facilitates leukocyte recruitment and may even function as an adhesion molecule when it is present in inflammatory exudates (31), its actions on the leukocyte recruitment cascade have not been detailed. We have therefore addressed the roles of both the endogenous and the recombinant protein on the inflammatory response initiated by two major pro-inflammatory cytokines.

The data presented show that endogenous Gal-3 is required for slow rolling of leukocytes in response to local treatment with the pro-inflammatory cytokines IL-1β and TNFα. The response to these cytokines differed however, in terms of the impact of Gal-3 on leukocyte emigration, providing further evidence of stimulus specific roles for this lectin. The reduced leukocyte emigration we observed in Gal-3$^{-/-}$ mice is in keeping with published results. Reduced monocyte, macrophage and neutrophil recruitment to the CNS occurs in a model of EAE (32) and despite conflicting reports using a thioglycollate broth model of peritonitis, reduced infiltration of neutrophils was observed at either day 1 or 4 after insult (33, 34). Farnworth *et al.* reported that Gal-3$^{-/-}$ mice exhibited more severe lung injury associated with reduced neutrophil recruitment at 15 h after *S. pneumoniae* infection: of interest, neutrophil recruitment in this model is independent of β_2-integrins (35). This reduction in extravasated neutrophils at 12-24 h was also reported by Nieminen *et al.,* who found that recruitment was unaffected in β_2-integrin-dependent *E. Coli*-driven lung infection in Gal-3$^{-/-}$ animals (36). These studies have led to the hypothesis that Gal-3 may function as *a bona fide* adhesion molecule in response to particular stimuli. Our data suggest that while this may be case, with discrepancies between the response observed to IL-1β versus TNFα, the role of Gal-3 extends beyond models in which the recruitment is β_2-integrin independent. The effects of Gal-3 on leukocyte recruitment we have identified here are not limited to neutrophils; Gal-3 expression is increased in murine lungs with allergic asthma and Gal-3$^{-/-}$

mice display reduced lung and airway eosinophilia in response to acute and chronic ovalbumin challenge, respectively (37). Further investigation showed endogenous Gal-3 is required for rolling of bone marrow-derived eosinophils on VCAM-1 and showed a trend to be required for stable adhesion on ICAM-1 under conditions of flow. This was in addition to its requirement for subsequent activation-induced morphological changes such as cell spreading and protrusion formation as well as intracellular Gal-3 being vital for eosinophil migration to eotaxin-1 in Transwells™ (38).

Our findings suggest stimulus-specific roles for Gal-3 as evidenced by the different responses we observed to IL-1β and TNFα in the absence of Gal-3. Since IL-1β activates the endothelia directly (24) the differences in leukocyte emigration quantified in Gal-3$^{-/-}$ mice suggest that endothelial function may be compromised in these animals, possibly in terms of their expression of CAMs and junctional adhesion molecules involved in transmigration. Our finding that Gal-3$^{-/-}$ endothelial cells express reduced ICAM-1 and E-selectin following IL-1β treatment; an outcome that would have direct consequences for IL-1β-induced slow rolling and possibly subsequent transmigration suggests that the function of the endothelium is defective in these mice. More recently, it was found that neutrophil transmigration elicited by IL-1β but not TNFα is protein-synthesis dependent and requires ICAM-2, JAM-A then PECAM-1 in distinct but sequential steps (24, 39). In future the expression of these molecules in Gal-3$^{-/-}$ endothelial cells should be assessed as well as their glycosylation pattern, since all three contain N-glycosylation sites (40–42). Also of interest to this study, IL-1β but not TNFα-induced neutrophil transmigration is dependent on α_6-integrin (43), which is recognised by HPA lectin, one of those found to exhibit reduced binding in Gal-3$^{-/-}$ cells.

Furthermore, Young *et al* showed that wild type neutrophils respond to TNFα by increasing their expression of β$_2$-integrin (CD18) and shedding L-selectin, in contrast to cells treated with IL-1β (24). Since Gal-3 is not thought to affect β$_2$-integrin-dependent leukocyte recruitment (36), CD11b, which forms Mac-1 with the β$_2$-integrin CD18, was investigated. Flow cytometric analysis showed that Gal-3$^{-/-}$ neutrophils express reduced PSGL-1 in response to TNFα, a finding that could have direct consequences for leukocyte slow rolling since PSGL-1 is a known ligand of E-selectin and these interactions support slow rolling in post-capillary venules (44). Also Gal-3$^{-/-}$ neutrophils express reduced CD11b basally and after TNFα treatment, though levels of L-selectin were comparable.

It is worth noting here that despite this altered cell adhesion molecule expression on both Gal-3$^{-/-}$ neutrophils and endothelial cells, levels of adhesion were unchanged in Gal-3$^{-/-}$ mice, both basally and after stimulation. Kubes *et al.* demonstrated that rolling needs to be reduced by approximately 90% to affect levels of leukocyte adhesion; these authors used a high dose of fucoidin, a sulphated homopolymer of fucose, to attain this level of reduction and determined the ensuing attenuation of reperfusion-induced leukocyte adhesion (45). Furthermore, in wild type mice treated with TNFα approximately 90% of rolling leukocytes progress to become adherent and in E-selectin$^{-/-}$ mice where rolling velocities remain high, 50% of the rolling leukocytes are still able to adhere (46). There are several further explanations, which might account for these differences. In the current study, we have only looked at CD11b expression and not CD11a and it has been shown in Mac-1 (CD11b)

knockout mice that adhesion is normal due to the presence of CD11a (47), indeed studies have shown that LFA-1 is the dominant of the two molecules with regards to neutrophil adhesion and migration (48). It is possible and likely that in vivo other adhesion molecules compensate for any reduction in ICAM-1 that might be present in Gal-3$^{-/-}$ mice. In support of this hypothesis, leukocyte trafficking is relatively normal in ICAM-1 deficient mice in a model of thioglycollate peritonitis (49), an effect that the authors proposed might be due to the ability of other adhesion molecules such as P- and E-selectin, LFA-1/ICAM-2 or α4β1 integrin. Interestingly optimal rolling in vivo is reliant on ICAM-1, which might be the reason why differences are observed in knockout mice with regards to rolling velocity rather than adhesion. Steeber et al (50) have shown that at later time-points during trauma-induced rolling in the cremaster (when P-selectin does not play such a dominant role) as well as in response to TNF-α stimulation, that rolling velocities are significantly increased in ICAM-1 KO mice compared to WT. These studies and data presented here highlight the complex yet distinct nature of each step in the leukocyte recruitment cascade.

Our results in the parallel-plate flow chamber extend the findings of previous studies, which have focused on the end phase of transmigration. By using intra-vital microscopy and the parallel plate flow chamber we have been able to identify defects at earlier stages of the leukocyte recruitment cascade, namely rolling and activation. We have shown that Gal-3$^{-/-}$ leukocytes did not capture to E-selectin and initiate downstream changes in their activation state and cell morphology. In order to investigate this further we examined the availability of E-selectin ligands in the absence of Gal-3 and determined that Gal-3$^{-/-}$ neutrophils displayed reduced HPA and PNA lectin binding, indicating that these cells have an altered cell surface glycophenotype. The importance of post-translational modification of E-selectin ligands to their functionality was recently demonstrated using mice lacking the polypeptide GalNAc transferase-1, which generates core-type O-glycan structures from GalNAc binding to threonine or serine residues in their protein backbone. Galnt-1$^{-/-}$ mice display reduced P- and E-selectin-mediated rolling, which in turn reduces adhesion and emigration of leukocytes in these animals; signalling through syk and thus integrin activation was unaffected, confirming that it is the ability of ligands to bind rather than downstream pathways, which are impaired (51). Of particular importance here, Saravanan *et al.* (2009) found that various glycogens were differentially expressed in Gal-3$^{-/-}$ mice undergoing a corneal model of wound-healing; these included glycosyltransferases and glycosidases that were down- or upregulated in order to produce less N-glycans and more O-glycans. For example, an enzyme involved in Gal-3 ligand synthesis, β3-galactotransferase 5 (β3GalT5), was downregulated whereas N-acetylgalactosaminyltransferases-3 and -7 (ppGalNAcTs-3 and -7) which initiate O-glycosylation, were upregulated (52).

It was important to observe that changes in lectin binding were specific with discreet alterations in HPA and PNA binding emerging from the assay analyses. HPA selectively binds to α-N-acetylgalactosamine residues and has been extensively studied as a marker of cancer cell metastasis (53). Another study highlighted the similar structure of HPA and sLe^x, hypothesising they may have overlapping but not identical glycotopes (54), supporting the notion we propose herein that reduced HPA binding indicates reduced selectin ligand binding. A putative receptor for PNA in keratinocytes is CD44, a known E-selectin ligand:

this leads us to suggest that although CD44 levels are not reduced in Gal-3$^{-/-}$ leukocytes, they may display reduced binding capacity due to altered glycosylation (55).

Overall our results suggest that there are defects in both the endothelial and haematopoietic compartments in Gal-3$^{-/-}$ mice. This is evidenced by the reduced recruitment of Gal-3$^{-/-}$ leukocytes in the in vitro flow assay as well as the greater defect in response to the endothelial-dependent stimulus IL-1β in vivo. One way to address this issue would be through the generation of bone marrow chimeras, however we would anticipate from our results that defects in trafficking would be observed when Gal-3 is absent from either compartment, particularly if a global loss of Gal-3 results in an altered cellular glycophenotype. One way to address this issue would be to generate conditional knockout mice, as this would enable the role of particular cellular sources of Gal-3 to be examined.

In the second part of this study, we have shown that exogenous Gal-3 elicits an inflammatory response alone, whereby local administration of recombinant Gal-3 to WT mice resulted in a dose-dependent reduction in rolling velocity associated with increased numbers of adherent and emigrated leukocytes, approximately half of which were Ly6G-positive neutrophils. Intrascrotal administration of Gal-3 to CX$_3$CR1$^{gfp/+}$ mice confirmed that approximately equal numbers of monocytes are also recruited in response to this lectin. These findings are supported by numerous *in vitro* studies where Gal-3 acts as a chemoattractant for human neutrophils and monocytes *in vitro* and induces their recruitment to a mouse air-pouch model (56). Studies have also examined the role of Gal-3 in murine models of *Streptococcal pneumoniae* lung infection; accumulation of Gal-3 in the lungs correlated with neutrophil emigration to the alveoli during infection and low levels of Gal-3 were bound to the neutrophil cell surface.

Our *in vivo* data has furthered our knowledge on the role of Gal-3 in leukocyte recruitment by extending its actions to monocyte recruitment as well as neutrophils. The effects of Gal-3 on monocyte migration have been further studied *in vitro* where this lectin promoted monocyte chemotaxis, a finding replicated for human macrophages (57). Of note, Melo *et al.* found that treatment of Gal-3 null sarcoma cells with recombinant Gal-3 increased migration on laminin suggesting that any defects in the cells could be rescued (58). This rescue effect was not apparent in the current study as treatment of Gal-3$^{-/-}$ leukocytes with physiological levels of recombinant Gal-3 in the *ex vivo* flow chamber assays was unable to reverse their phenotype and did not increase their capture to E-selectin under conditions of flow. Taken together with our findings that intravenous administration of Gal-3 did not affect leukocyte recruitment, this provides further evidence that, at least in these models and with the concentrations used in this study, a global lack of Gal-3 results in impaired leukocyte function *in vivo*.

Rather than acting directly on the leukocytes, the effect of exogenously delivered Gal-3 were indirect, and lead to increased mRNA for IL-1β, TNFα, KC, MCP-1 and IL-6 in the cremaster preparations. With the exception of IL-1β, these results were confirmed by proteome profile, which also revealed higher levels of IFNγ, MIP-2 and MIP-1α post-Gal-3. These data point to stromal cells as the plausible target for Gal-3 to initiate a local inflammatory response. This is consistent with reports in the literature. Since levels of Gal-3

are increased at sites of joint destruction in RA, Filer *et al.* investigated the effect of exogenous Gal-3 treatment of human synovial fibroblasts, which increased their production of IL-6, GM-CSF, TNFα and MMP-3 as well as the neutrophil chemoattractant IL-8 and the monocyte chemoattractants MCP-1, MIP-1α and RANTES. The authors established that autocrine TNFα stimulation was not the cause of this release; in fact ERK MAPK activation occurred within 5 min and JNK, p38 MAPK and Akt phosphorylation was evident at 15 min as well as activation of NFκB (59). The activation of PI3K by Gal-3 has also been demonstrated in macrophages, which is often associated with chemokine production by stromal cells (60) as well as E-selectin-dependent neutrophil rolling and trafficking (61), both cell types that are abundant in the cremaster muscle.

Taken together these results confirm that Gal-3 is a multi-faceted molecule that exhibits modulatory properties on many aspects of the inflammatory response; based on our results, we propose the following model (Fig. 7.) whereby the endogenous protein functions to potentiate the inflammatory response as evidenced by reduced adhesion molecule expression and an altered glycosylation profile culminating in a lack of slow rolling and reduced emigration in response to IL-1β. This is in contrast to exogenously administered Gal-3, which evokes a tissue-restricted circuit by acting on stromal cells (plausible ones are fibroblasts, macrophages and endothelial cells) resulting in an enhanced pro-inflammatory state that culminates in increased levels of leukocyte trafficking. We propose that full definition of the roles for Gal-3 in controlling vascular inflammation can help in designing novel approaches for therapeutic benefit.

Supplementary Material

Refer to Web version on PubMed Central for supplementary material.

Acknowledgements

References

1. Gilroy DW, Lawrence T, Perretti M, Rossi AG. Inflammatory resolution: new opportunities for drug discovery. Nat Rev Drug Discov. 2004; 3:401–416. [PubMed: 15136788]

2. Serhan CN, Brain SD, Buckley CD, Gilroy DW, Haslett C, O'Neill LA, Perretti M, Rossi AG, Wallace JL. Resolution of inflammation: state of the art, definitions and terms. Faseb J. 2007; 21:325–332. [PubMed: 17267386]

3. Hollingsworth JW, Siegel ER, Creasey WA. Granulocyte survival in synovial exudate of patients with rheumatoid arthritis and other inflammatory joint diseases. The Yale journal of biology and medicine. 1967; 39:289–296. [PubMed: 6034277]

4. Ley K, Laudanna C, Cybulsky MI, Nourshargh S. Getting to the site of inflammation: the leukocyte adhesion cascade updated. Nature reviews Immunology. 2007; 7:678–689.

5. Luster AD, Alon R, von Andrian UH. Immune cell migration in inflammation: present and future therapeutic targets. Nature immunology. 2005; 6:1182–1190. [PubMed: 16369557]

6. Barondes SH, Castronovo V, Cooper DN, Cummings RD, Drickamer K, Feizi T, Gitt MA, Hirabayashi J, Hughes C, Kasai K, et al. Galectins: a family of animal beta-galactoside-binding lectins. Cell. 1994; 76:597–598. [PubMed: 8124704]

7. Cummings RD, Trowbridge IS, Kornfeld S. A mouse lymphoma cell line resistant to the leukoagglutinating lectin from Phaseolus vulgaris is deficient in UDP-GlcNAc: alpha-D-mannoside beta 1,6 N-acetylglucosaminyltransferase. The Journal of biological chemistry. 1982; 257:13421–13427. [PubMed: 6216250]

8. Ohshima S, Kuchen S, Seemayer CA, Kyburz D, Hirt A, Klinzing S, Michel BA, Gay RE, Liu FT, Gay S, Neidhart M. Galectin 3 and its binding protein in rheumatoid arthritis. Arthritis Rheum. 2003; 48:2788–2795. [PubMed: 14558084]

9. de Boer RA, Lok DJ, Jaarsma T, van der Meer P, Voors AA, Hillege HL, van Veldhuisen DJ. Predictive value of plasma galectin-3 levels in heart failure with reduced and preserved ejection fraction. Annals of medicine. 2011; 43:60–68. [PubMed: 21189092]

10. Lee YJ, Kang SW, Song JK, Park JJ, Bae YD, Lee EY, Lee EB, Song YW. Serum galectin-3 and galectin-3 binding protein levels in Behcet's disease and their association with disease activity. Clinical and experimental rheumatology. 2007; 25:S41–45.

11. Sato S, Ouellet N, Pelletier I, Simard M, Rancourt A, Bergeron MG. Role of galectin-3 as an adhesion molecule for neutrophil extravasation during streptococcal pneumonia. J Immunol. 2002; 168:1813–1822. [PubMed: 11823514]

12. Cooper D, Norling LV, Perretti M. Novel insights into the inhibitory effects of Galectin-1 on neutrophil recruitment under flow. Journal of leukocyte biology. 2008; 83:1459–1466. [PubMed: 18372340]

13. Swamydas M, Lionakis MS. Isolation, purification and labeling of mouse bone marrow neutrophils for functional studies and adoptive transfer experiments. Journal of visualized experiments: JoVE. 2013; e50586

14. Reynolds LE, Hodivala-Dilke KM. Primary mouse endothelial cell culture for assays of angiogenesis. Methods Mol Med. 2006; 120:503–509. [PubMed: 16491622]

15. Pfaffl MW. A new mathematical model for relative quantification in real-time RT-PCR. Nucleic acids research. 2001; 29:e45. [PubMed: 11328886]

16. Dinarello CA. A clinical perspective of IL-1β as the gatekeeper of inflammation. Eur J Immunol. 2011; 41:1203–1217. [PubMed: 21523780]

17. Dinarello CA. Proinflammatory Cytokines. CHEST Journal. 2000; 118:503–508.

18. Schiff M. Role of interleukin 1 and interleukin 1 receptor antagonist in the mediation of rheumatoid arthritis. Ann Rheum Dis. 2000; 59:i103–108. [PubMed: 11053099]

19. Kollias G, Douni E, Kassiotis G, Kontoyiannis D. The function of tumour necrosis factor and receptors in models of multi-organ inflammation, rheumatoid arthritis, multiple sclerosis and inflammatory bowel disease. Ann Rheum Dis. 1999; 58(Suppl 1):I32–39. [PubMed: 10577971]

20. Rampart M, U o A; (UIA), Fiers W, S U o G; (RUG), Smet Wd, Innogenetics; Herman AG, U o A. (UIA). Different pro-inflammatory profiles of interleukin 1 (IL 1) and tumor necrosis factor (TNF) in an in vivo model of inflammation. Agents and Actions. 1989; 26:186–188. [PubMed: 2785335]

21. Kunkel EJ, Ley K. Distinct phenotype of E-selectin-deficient mice. E-selectin is required for slow leukocyte rolling in vivo. Circ Res. 1996; 79:1196–1204. [PubMed: 8943958]

22. Simon SI, Hu Y, Vestweber D, Smith CW. Neutrophil tethering on E-selectin activates beta 2 integrin binding to ICAM-1 through a mitogen-activated protein kinase signal transduction pathway. J Immunol. 2000; 164:4348–4358. [PubMed: 10754335]

23. CFG. Galectin 3 null mouse phenotype. 2013

24. Young RE, Thompson RD, Nourshargh S. Divergent mechanisms of action of the inflammatory cytokines interleukin 1-beta and tumour necrosis factor-alpha in mouse cremasteric venules. Br J Pharmacol. 2002; 137:1237–1246. [PubMed: 12466233]

25. Kuwabara I, Liu FT. Galectin-3 promotes adhesion of human neutrophils to laminin. J Immunol. 1996; 156:3939–3944. [PubMed: 8621934]

26. Nieminen J, Kuno A, Hirabayashi J, Sato S. Visualization of galectin-3 oligomerization on the surface of neutrophils and endothelial cells using fluorescence resonance energy transfer. J Biol Chem. 2007; 282:1374–1383. [PubMed: 17082191]

27. Yang RY, Hsu DK, Liu FT. Expression of galectin-3 modulates T-cell growth and apoptosis. Proceedings of the National Academy of Sciences of the United States of America. 1996; 93:6737–6742. [PubMed: 8692888]

28. Fukumori T, Takenaka Y, Yoshii T, Kim HR, Hogan V, Inohara H, Kagawa S, Raz A. CD29 and CD7 mediate galectin-3-induced type II T-cell apoptosis. Cancer research. 2003; 63:8302–8311. [PubMed: 14678989]

29. Bhaumik P, St-Pierre G, Milot V, St-Pierre C, Sato S. Galectin-3 facilitates neutrophil recruitment as an innate immune response to a parasitic protozoa cutaneous infection. J Immunol. 2013; 190:630–640. [PubMed: 23241887]

30. Nieminen J, St-Pierre C, Bhaumik P, Poirier F, Sato S. Role of galectin-3 in leukocyte recruitment in a murine model of lung infection by Streptococcus pneumoniae. J Immunol. 2008; 180:2466–2473. [PubMed: 18250456]

31. Sato S, Ouellet N, Pelletier I, Simard M, Rancourt A, Bergeron MG. Role of galectin-3 as an adhesion molecule for neutrophil extravasation during streptococcal pneumonia. J Immunol. 2002; 168:1813–1822. [PubMed: 11823514]

32. Jiang HR, Al Rasebi Z, Mensah-Brown E, Shahin A, Xu D, Goodyear CS, Fukada SY, Liu FT, Liew FY, Lukic ML. Galectin-3 deficiency reduces the severity of experimental autoimmune encephalomyelitis. J Immunol. 2009; 182:1167–1173. [PubMed: 19124760]

33. Hsu DK, Yang RY, Pan Z, Yu L, Salomon DR, Fung-Leung WP, Liu FT. Targeted disruption of the galectin-3 gene results in attenuated peritoneal inflammatory responses. Am J Pathol. 2000; 156:1073–1083. [PubMed: 10702423]

34. Colnot C, Ripoche MA, Milon G, Montagutelli X, Crocker PR, Poirier F. Maintenance of granulocyte numbers during acute peritonitis is defective in galectin-3-null mutant mice. Immunology. 1998; 94:290–296. [PubMed: 9767409]

35. Farnworth SL, Henderson NC, Mackinnon AC, Atkinson KM, Wilkinson T, Dhaliwal K, Hayashi K, Simpson AJ, Rossi AG, Haslett C, Sethi T. Galectin-3 reduces the severity of pneumococcal pneumonia by augmenting neutrophil function. Am J Pathol. 2008; 172:395–405. [PubMed: 18202191]

36. Nieminen J, St-Pierre C, Bhaumik P, Poirier F, Sato S. Role of galectin-3 in leukocyte recruitment in a murine model of lung infection by Streptococcus pneumoniae. J Immunol. 2008; 180:2466–2473. [PubMed: 18250456]

37. Ge XN, Bahaie NS, Kang BN, Hosseinkhani MR, Ha SG, Frenzel EM, Liu FT, Rao SP, Sriramarao P. Allergen-induced airway remodeling is impaired in galectin-3-deficient mice. J Immunol. 2010; 185:1205–1214. [PubMed: 20543100]

38. Ge XN, Ha SG, Liu FT, Rao SP, Sriramarao P. Eosinophil-expressed galectin-3 regulates cell trafficking and migration. Front Pharmacol. 2013; 4:37. [PubMed: 23576987]

39. Woodfin A, Voisin MB, Imhof BA, Dejana E, Engelhardt B, Nourshargh S. Endothelial cell activation leads to neutrophil transmigration as supported by the sequential roles of ICAM-2, JAM-A, and PECAM-1. Blood. 2009; 113:6246–6257. [PubMed: 19211506]

40. Koenen RR, Pruessmeyer J, Soehnlein O, Fraemohs L, Zernecke A, Schwarz N, Reiss K, Sarabi A, Lindbom L, Hackeng TM, Weber C, et al. Regulated release and functional modulation of junctional adhesion molecule A by disintegrin metalloproteinases. Blood. 2009; 113:4799–4809. [PubMed: 19258599]

41. Feduska JM, Garcia PL, Brennan SB, Bu S, Council LN, Yoon KJ. N-glycosylation of ICAM-2 is required for ICAM-2-mediated complete suppression of metastatic potential of SK-N-AS neuroblastoma cells. BMC Cancer. 2013; 13:261. [PubMed: 23714211]

42. Newton JP, Hunter AP, Simmons DL, Buckley CD, Harvey DJ. CD31 (PECAM-1) exists as a dimer and is heavily N-glycosylated. Biochem Biophys Res Commun. 1999; 261:283–291. [PubMed: 10425179]

43. Dangerfield JP, Wang S, Nourshargh S. Blockade of alpha6 integrin inhibits IL-1beta- but not TNF-alpha-induced neutrophil transmigration in vivo. J Leukoc Biol. 2005; 77:159–165. [PubMed: 15539457]

44. Norman KE, Katopodis AG, Thoma G, Kolbinger F, Hicks AE, Cotter MJ, Pockley AG, Hellewell PG. P-selectin glycoprotein ligand-1 supports rolling on E- and P-selectin in vivo. Blood. 2000; 96:3585–3591. [PubMed: 11071658]

45. Kubes P, Jutila M, Payne D. Therapeutic potential of inhibiting leukocyte rolling in ischemia/ reperfusion. 1995

46. Kunkel EJ, Dunne JL, Ley K. Leukocyte arrest during cytokine-dependent inflammation in vivo. J Immunol. 2000; 164:3301–3308. [PubMed: 10706723]

47. Lu H, Smith CW, Perrard J, Bullard D, Tang L, Shappell SB, Entman ML, Beaudet AL, Ballantyne CM. LFA-1 is sufficient in mediating neutrophil emigration in Mac-1-deficient mice. The Journal of clinical investigation. 1997; 99:1340–1350. [PubMed: 9077544]

48. Ding ZM, Babensee JE, Simon SI, Lu H, Perrard JL, Bullard DC, Dai XY, Bromley SK, Dustin ML, Entman ML, Smith CW, et al. Relative contribution of LFA-1 and Mac-1 to neutrophil adhesion and migration. J Immunol. 1999; 163:5029–5038. [PubMed: 10528208]

49. Steeber DA, Tang ML, Green NE, Zhang XQ, Sloane JE, Tedder TF. Leukocyte entry into sites of inflammation requires overlapping interactions between the L-selectin and ICAM-1 pathways. J Immunol. 1999; 163:2176–2186. [PubMed: 10438959]

50. Steeber DA, Campbell MA, Basit A, Ley K, Tedder TF. Optimal selectin-mediated rolling of leukocytes during inflammation in vivo requires intercellular adhesion molecule-1 expression. Proceedings of the National Academy of Sciences of the United States of America. 1998; 95:7562–7567. [PubMed: 9636189]

51. Block H, Ley K, Zarbock A. Severe impairment of leukocyte recruitment in ppGalNAcT-1-deficient mice. J Immunol. 2012; 188:5674–5681. [PubMed: 22544932]

52. Saravanan C, Cao Z, Head SR, Panjwani N. Detection of differentially expressed wound-healing-related glycogenes in galectin-3-deficient mice. Invest Ophthalmol Vis Sci. 2009; 50:5690–5696. [PubMed: 19643959]

53. Rambaruth ND, Greenwell P, Dwek MV. The lectin Helix pomatia agglutinin recognizes O-GlcNAc containing glycoproteins in human breast cancer. Glycobiology. 2012; 22:839–848. [PubMed: 22322011]

54. Kohler S, Ullrich S, Richter U, Schumacher U. E-/P-selectins and colon carcinoma metastasis: first in vivo evidence for their crucial role in a clinically relevant model of spontaneous metastasis formation in the lung. Br J Cancer. 2010; 102:602–609. [PubMed: 20010946]

55. Hudson DL, Sleeman J, Watt FM. CD44 is the major peanut lectin-binding glycoprotein of human epidermal keratinocytes and plays a role in intercellular adhesion. J Cell Sci. 1995; 108(Pt 5): 1959–1970. [PubMed: 7544799]

56. Sano H, Hsu DK, Yu L, Apgar JR, Kuwabara I, Yamanaka T, Hirashima M, Liu FT. Human galectin-3 is a novel chemoattractant for monocytes and macrophages. J Immunol. 2000; 165:2156–2164. [PubMed: 10925302]

57. Danella Polli C, Alves Toledo K, Franco LH, Sammartino Mariano V, de Oliveira LL, Soares Bernardes E, Roque-Barreira MC, Pereira-da-Silva G. Monocyte Migration Driven by Galectin-3 Occurs through Distinct Mechanisms Involving Selective Interactions with the Extracellular Matrix. ISRN Inflamm. 2013; 2013:259256. [PubMed: 24049657]

58. Melo FH, Butera D, Junqueira Mde S, Hsu DK, da Silva AM, Liu FT, Santos MF, Chammas R. The promigratory activity of the matricellular protein galectin-3 depends on the activation of PI-3 kinase. PLoS One. 2011; 6:e29313. [PubMed: 22216245]

59. Filer A, Bik M, Parsonage GN, Fitton J, Trebilcock E, Howlett K, Cook M, Raza K, Simmons DL, Thomas AM, Salmon M, et al. Galectin 3 induces a distinctive pattern of cytokine and chemokine production in rheumatoid synovial fibroblasts via selective signaling pathways. Arthritis Rheum. 2009; 60:1604–1614. [PubMed: 19479862]

60. MacKinnon AC, Farnworth SL, Hodkinson PS, Henderson NC, Atkinson KM, Leffler H, Nilsson UJ, Haslett C, Forbes SJ, Sethi T. Regulation of alternative macrophage activation by galectin-3. J Immunol. 2008; 180:2650–2658. [PubMed: 18250477]

61. Puri KD, Doggett TA, Huang CY, Douangpanya J, Hayflick JS, Turner M, Penninger J, Diacovo TG. The role of endothelial PI3Kgamma activity in neutrophil trafficking. Blood. 2005; 106:150–157. [PubMed: 15769890]
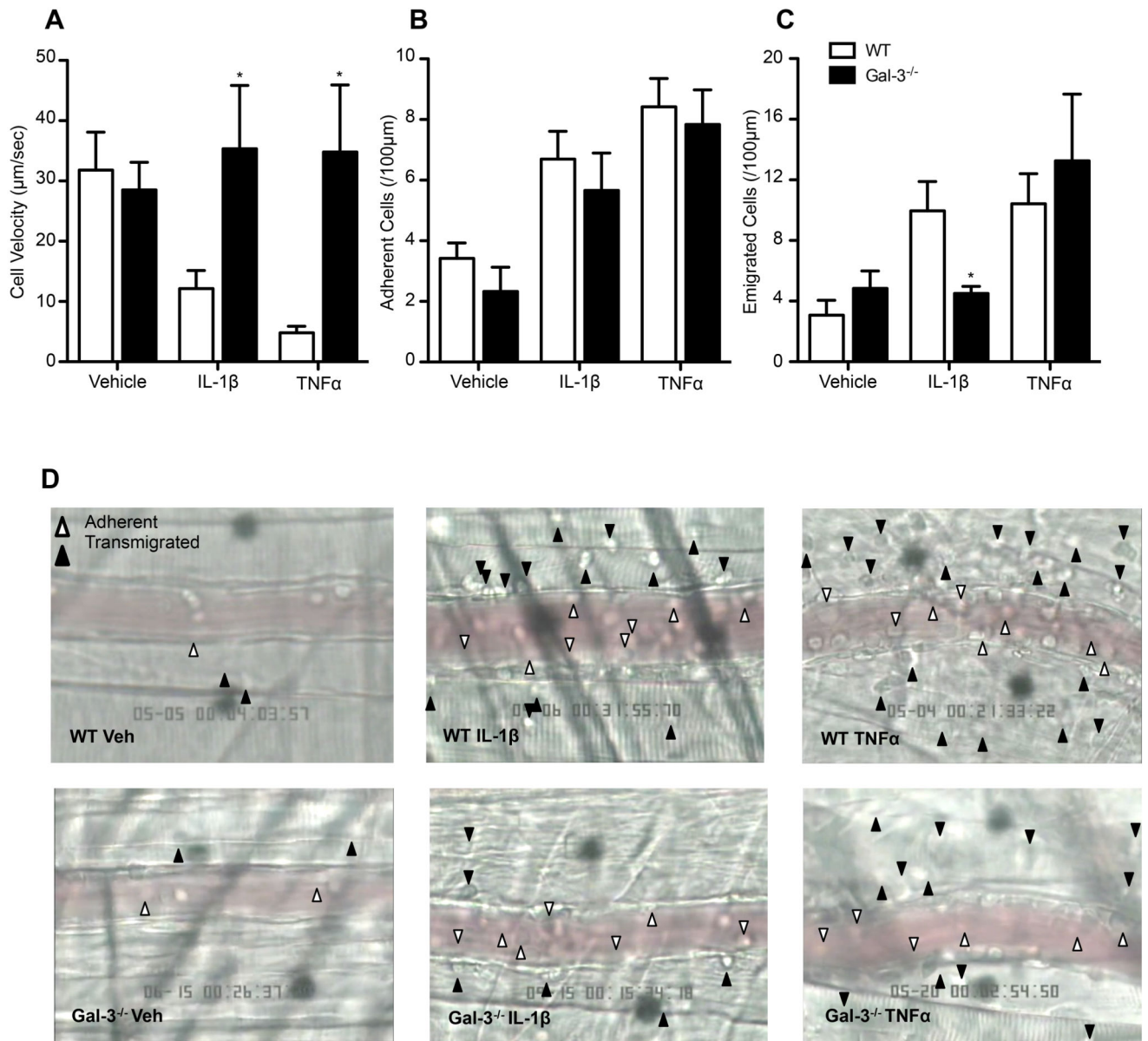
Fig. 1. Endogenous Gal-3 is required for leukocyte slow rolling in response to TNFα and IL-1β and leukocyte emigration in response to IL-1β in post-capillary venules.
Cremasteric post-capillary venules of C57BL/6 or Gal-3$^{-/-}$ mice were analysed by intravital microscopy following intrascrotal injection of TNFα (300ng) or IL-1β (30ng) 4 hours prior to exteriorisation. (A) leukocyte rolling velocity; (B) no. of adherent leukocytes (>30s); (C) no. of emigrated leukocytes. All data were obtained from segments of 100μm in 3-5 vessels per mouse and 3-5 mice per group. Results are expressed as mean±SEM for all parameters analysed. Statistical significance was assessed by two-way ANOVA and with Bonferroni's multiple comparison post-test; denoted by asterisks * P<0.05. (D) Representative images from vessels of C57BL/6 (upper panel) or Gal-3$^{-/-}$ mice (lower panel) following vehicle, IL-1β or TNFα treatment show rolling, adherent and emigrated leukocytes.
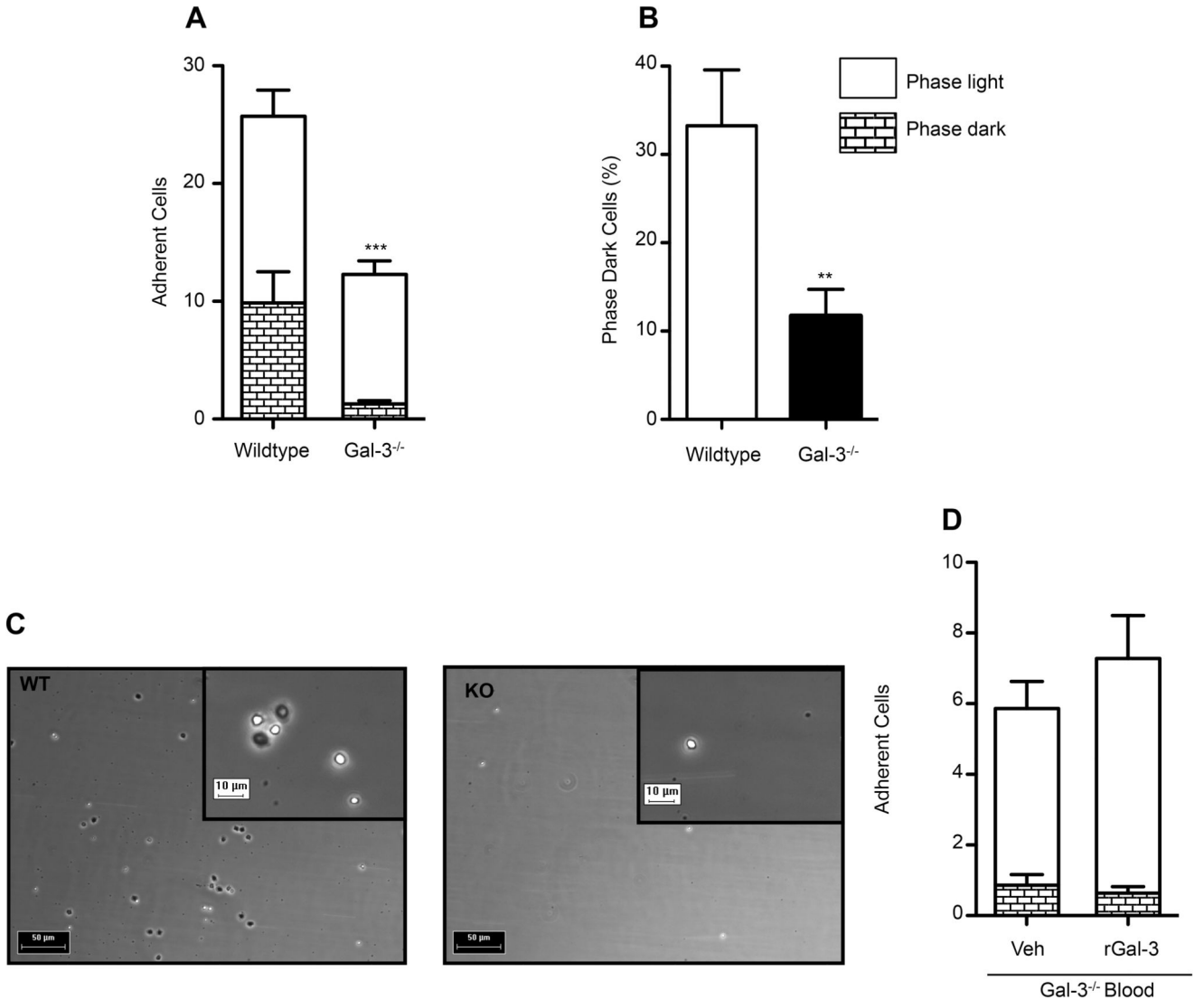
Fig. 2. Leukocyte binding to E-selectin and subsequent cellular morphological changes are disrupted in the absence of endogenous Gal-3

Murine leukocyte interactions with recombinant E-selectin were examined under conditions of flow. C57BL/6 or Gal-3$^{-/-}$ whole blood was collected by cardiac puncture and diluted in HBSS. Blood was flown for 3mins at 1.010ml/min, followed by 1min HBSS. Videos of 10s were captured for a total of 4-6 frames per mouse and 3 mice per group. Captured leukocytes in each frame were quantified and classified as phase dark or phase light according to their cellular morphology. The no. of adherent cells were quantified (A) and the percentage of cells transitioning to phase dark was calculated for each genotype (B). (C) Representative stills taken from C57BL/6 (left panel) or Gal-3$^{-/-}$ (right panel) experiments, scale 50μm; higher magnification shown in inset, scale 10μm. (D) Gal-3$^{-/-}$ whole blood was pre-treated for 15min at 37°C with recombinant Gal-3 (rGal-3; 10ng/mL) prior to flow. Results are expressed as mean±SEM. Significance was assessed using an unpaired student's t-test, denoted by asterisks * $P < 0.05$.
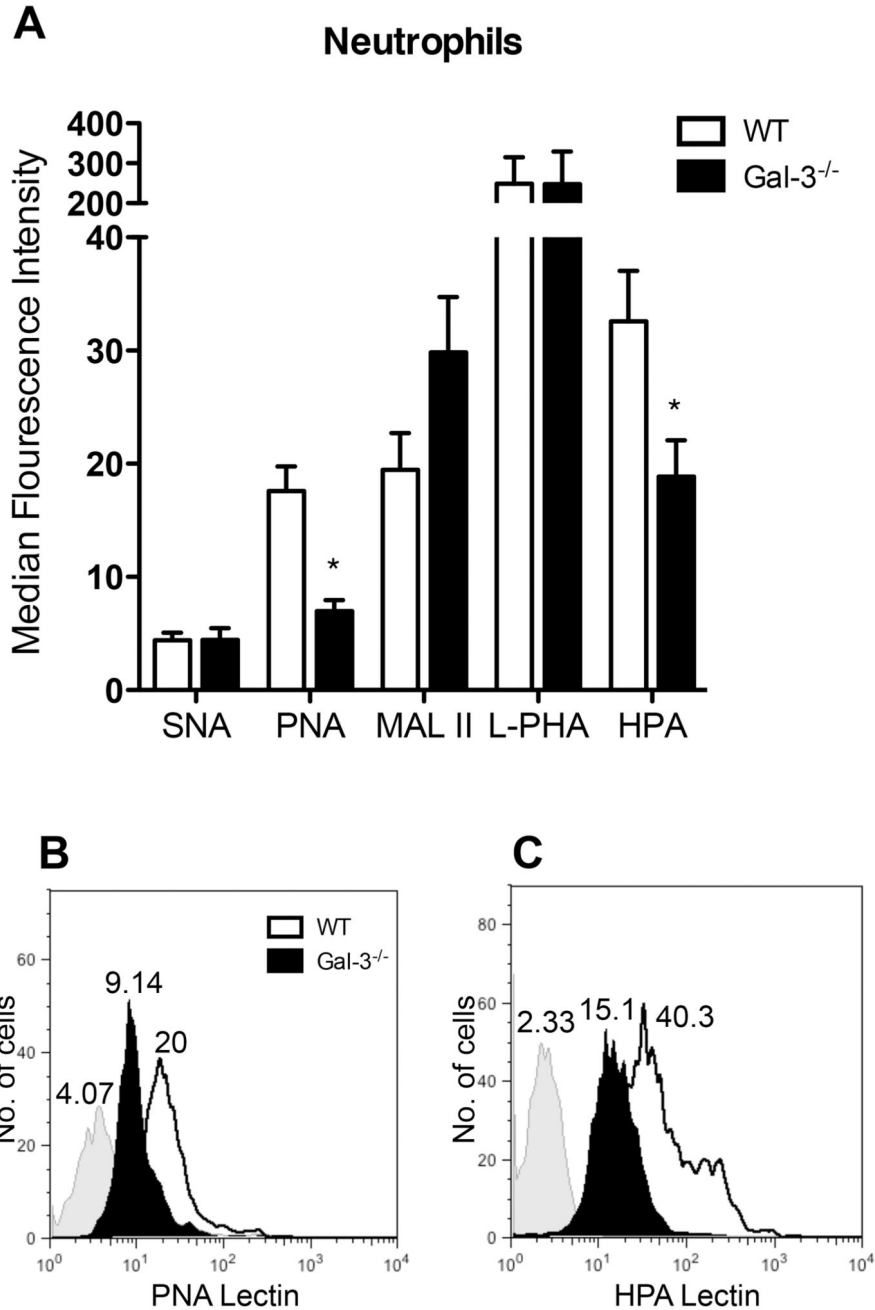
Fig. 3. Murine neutrophils display reduced PNA and HPA lectin binding sites on their cell surface.

Wild type or Gal-3$^{-/-}$ whole blood was collected by cardiac puncture before analysis by flow cytometry. (A) Ly-6g positive neutrophils were assessed for their ability to bind the lectins SNA, PNA, MALII, L-PHA and HPA by flow cytometry. (B) Representative histogram plot showing PNA lectin binding on wild type and Gal-3$^{-/-}$ neutrophils, with isotype control (grey). (C) Representative histogram plot showing HPA lectin binding on wild type and Gal-3$^{-/-}$ neutrophils, with isotype control (grey). Results are expressed as mean±SEM of 3-6

mice per group. Significance was assessed using an unpaired student's t-test, denoted by asterisks * P<0.05.
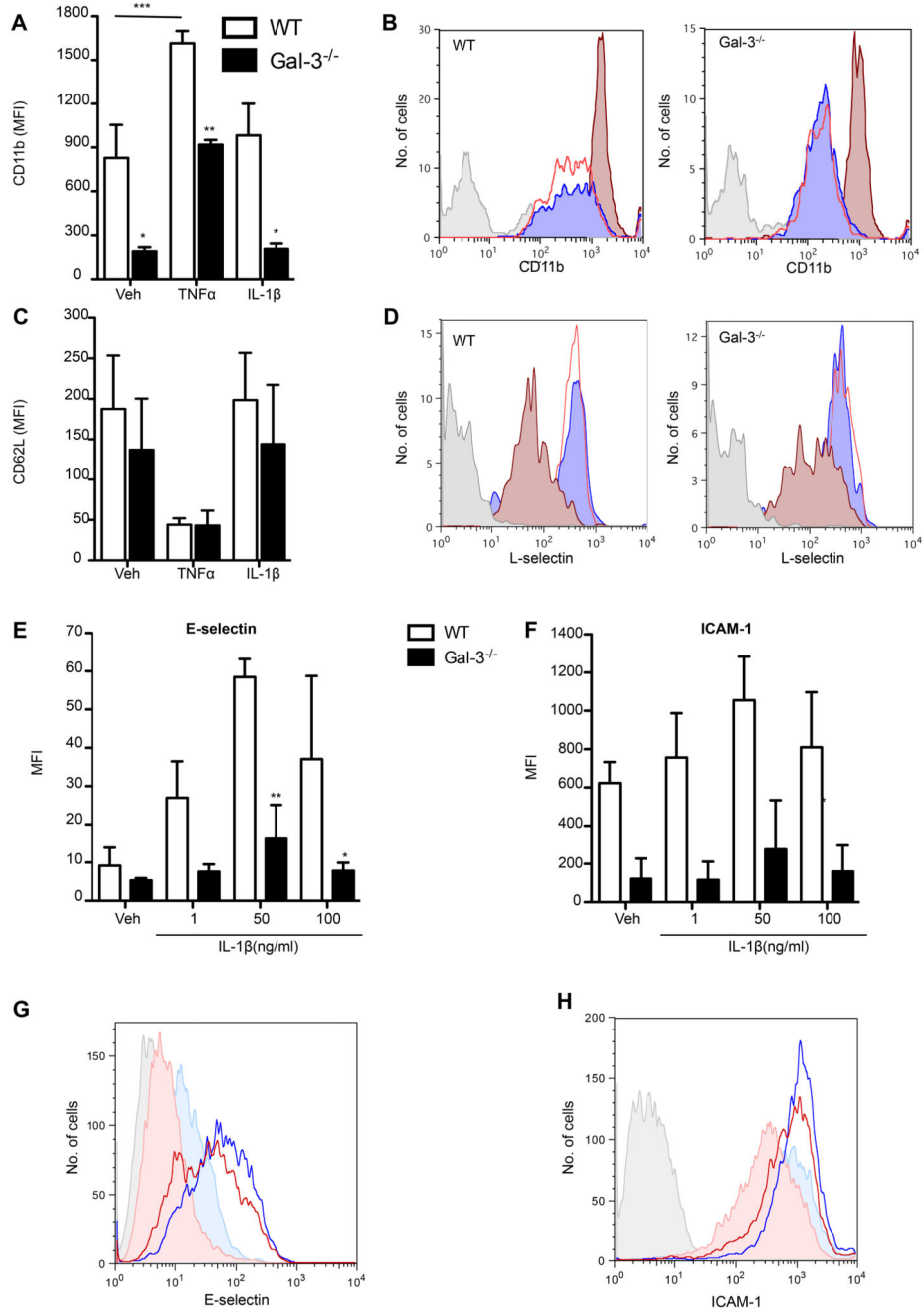
**Fig. 4. Cells lacking endogenous Gal-3 display altered ligand expression following activation with TNFα and IL-1β.**

(A-D) Wild type or Gal-3^{-/-} whole blood was treated for 10min at 37°C with TNFα (50ng/mL) or IL-1β (50ng/mL) and CD11b (A) and L-selectin (C) surface expression was assessed by flow cytometry. (B, D) Representative histogram plots of wild type and Gal-3^{-/-} neutrophils stained for isotype control (grey) or CD11b (B) or L-selectin (D) after treatment with vehicle (blue), IL-1β (red line) or TNFα (dark red). (E-F) Confluent wild type and Gal-3^{-/-} mEC were treated for 4h with IL-1β (1, 50, 100ng/mL) prior to analysis by flow cytometry. Representative histogram plots showing isotype control (grey tinted), vehicle

(PBS) treated wild type cells (filled pale blue), IL-1β (50ng/mL)-treated wild type cells (blue line), vehicle (PBS) treated Gal-3$^{-/-}$ cells (filled pale red) and IL-1β (50ng/mL)-treated Gal-3$^{-/-}$ cells (red line) stained for (E) E-selectin and (F) ICAM-1. Results are expressed as mean±SEM of 2-4 mice per group, significance was assessed by two-way ANOVA and Bonferroni's multiple comparison post-test, denoted by asterisks * P<0.05, ** P<0.01 and *** P<0.001.
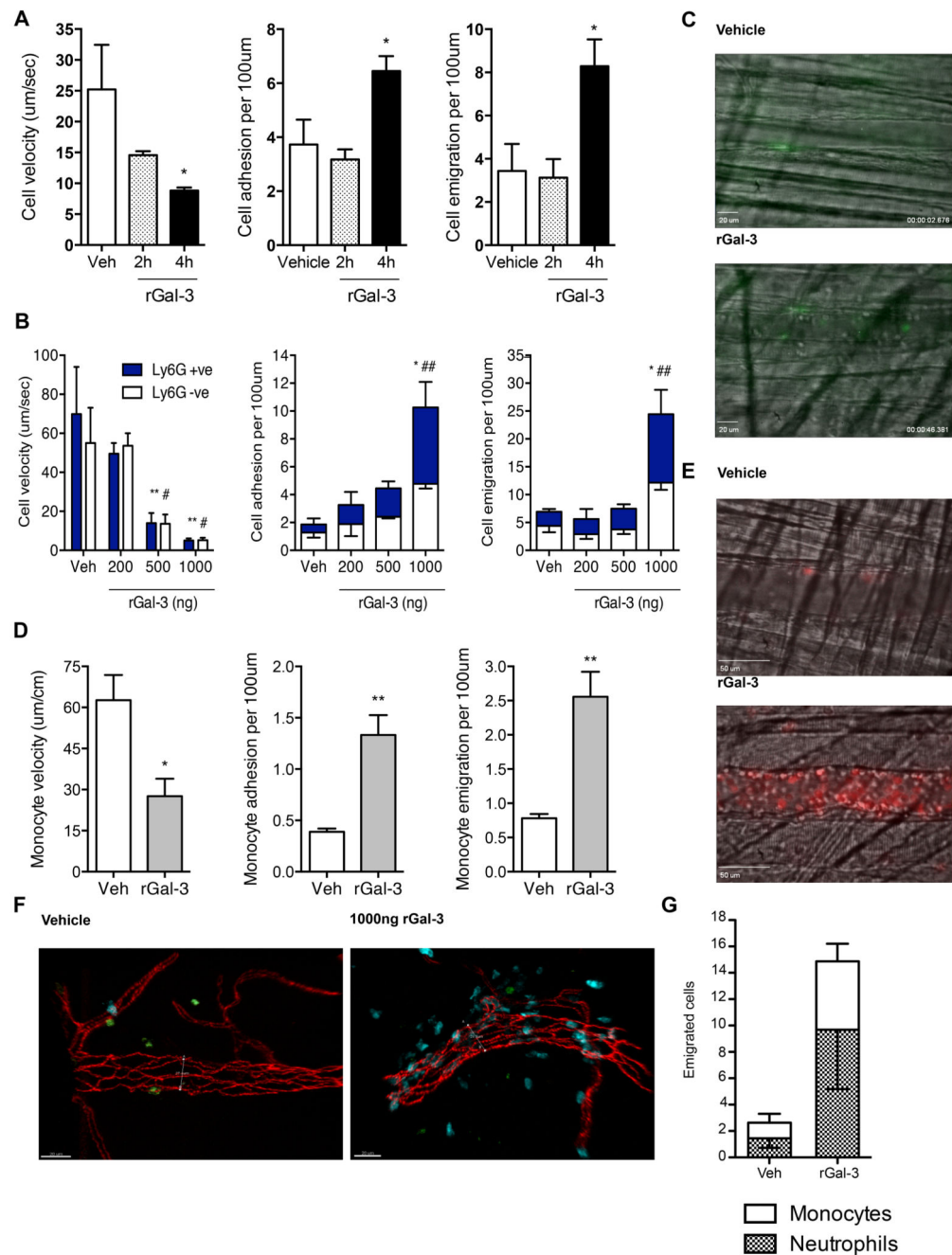
Fig. 5. Administration of recombinant Gal-3 results in neutrophil and monocyte recruitment to post-capillary venules.

Cremasteric post-capillary venules of C57BL/6 mice were analysed by intravital microscopy following intrascrotal injection of rGal-3 (500ng) 2 or 4 hours prior to exteriorisation. (A) leukocyte rolling velocity, no. of adherent leukocytes (>30s) and no. of emigrated leukocytes. Cremasteric post-capillary venules of CX$_3$CR1$^{gfp/+}$ mice were assessed 4h after intrascrotal injection of rGal-3 (1000ng) and GFP-positive monocyte rolling velocity, adhesion and emigration was analysed (B). (C) Representative images from vessels of CX$_3$CR1$^{gfp/+}$ mice following vehicle or rGal-3 administration, where monocytes are GFP-

positive (green). (D) The cremasteric microcirculation in C57BL/6 mice was assessed 4h after intrascrotal injection of rGal-3 (200-1000ng) and i.v. administration of anti-mouse Ly-6G (2μg) to label murine neutrophils. Ly-6G positive cells are shown in the filled columns and Ly-6G negative cells in the empty columns. (E) Representative images from vessels of C57BL/6 mice following vehicle or rGal-3 administration, where neutrophils are stained with anti-mouse Ly-6G (red). (F) Cremasters from $CX_3CR1^{gfp/+}$ mice treated intrascrotally for 4h with rGal-3 (1000ng) were exteriorised before analysis by confocal microscopy. Representative images from vehicle and rGal-3 -treated mice; vessels are stained using VE-Cadherin (Red), MRP14 positive neutrophils are blue and GFP positive monocytes are green. (G) Emigrated neutrophils and monocytes were quantified. All data obtained from segments of 100μm in 3-5 vessels per mouse and 3-5 mice per group. Results are expressed as mean±SEM for all parameters analysed. Statistical significance was assessed by one- or two-way ANOVA and with Tukey's multiple comparison post-test or unpaired student's t-tests; denoted by asterisks * $P<0.05$. and ** $P<0.01$ and # $P<0.05$ and ## $P<0.01$ between Ly-6G+ve bars.
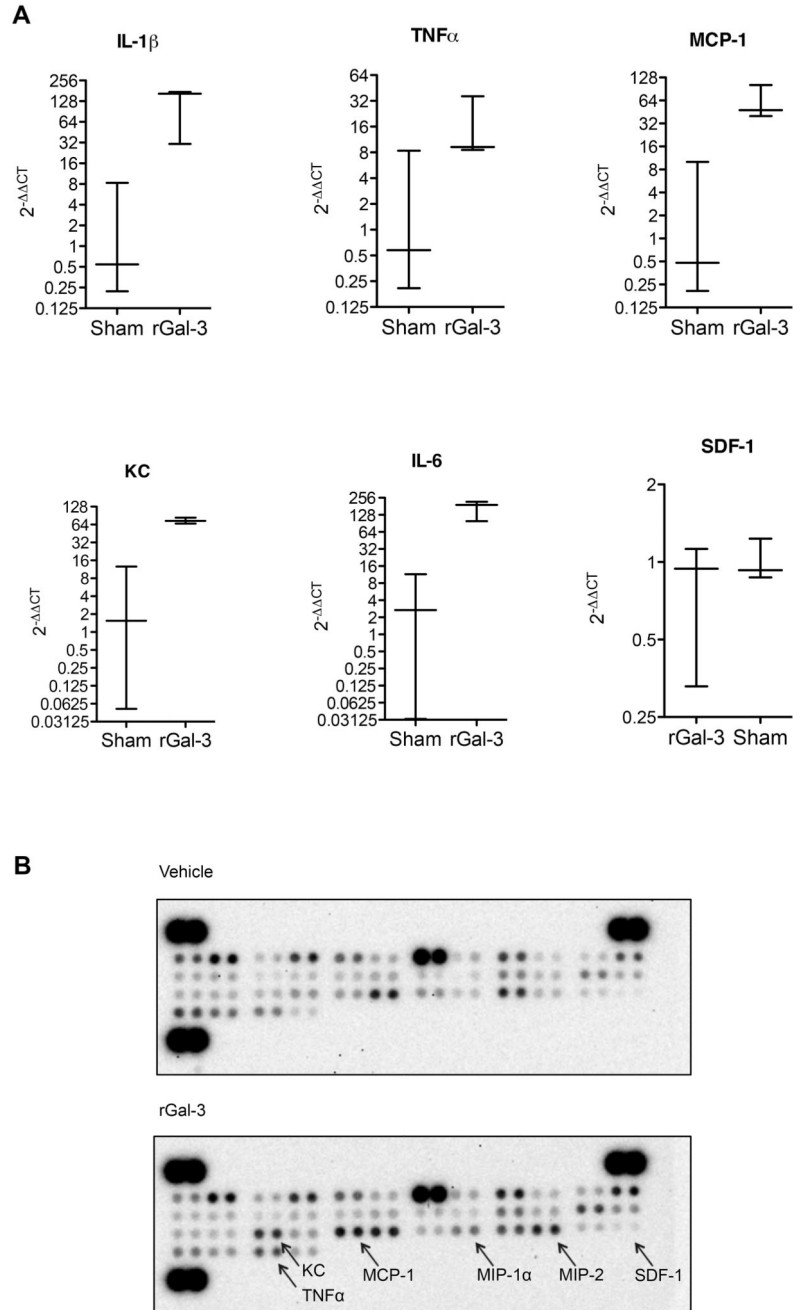
Fig. 6. Administration of recombinant Gal-3 results in increased pro-inflammatory cytokine and chemokine expression in the local tissue microenvironment

The cremasteric tissue of C57BL/6 mice was assessed 4h after intrascrotal injection of PBS or recombinant Gal-3 (1000ng). (A) Gene expression of IL-1β, TNFα, KC, MCP-1, IL-6 and SDF-1 following exogenous Gal-3 treatment. Results are expressed as $2^{-\Delta\Delta CT}$ where gene expression is normalised to an internal housekeeping gene (GAPDH) and then normalised once more to the sham cremasters. Results are displayed as mean±SEM of 2-3 mice per group. (B) Protein content was assessed using the mouse cytokine array panel A

Proteome Profiler™ using tissue homogenates from cremasters treated with exogenous Gal-3.
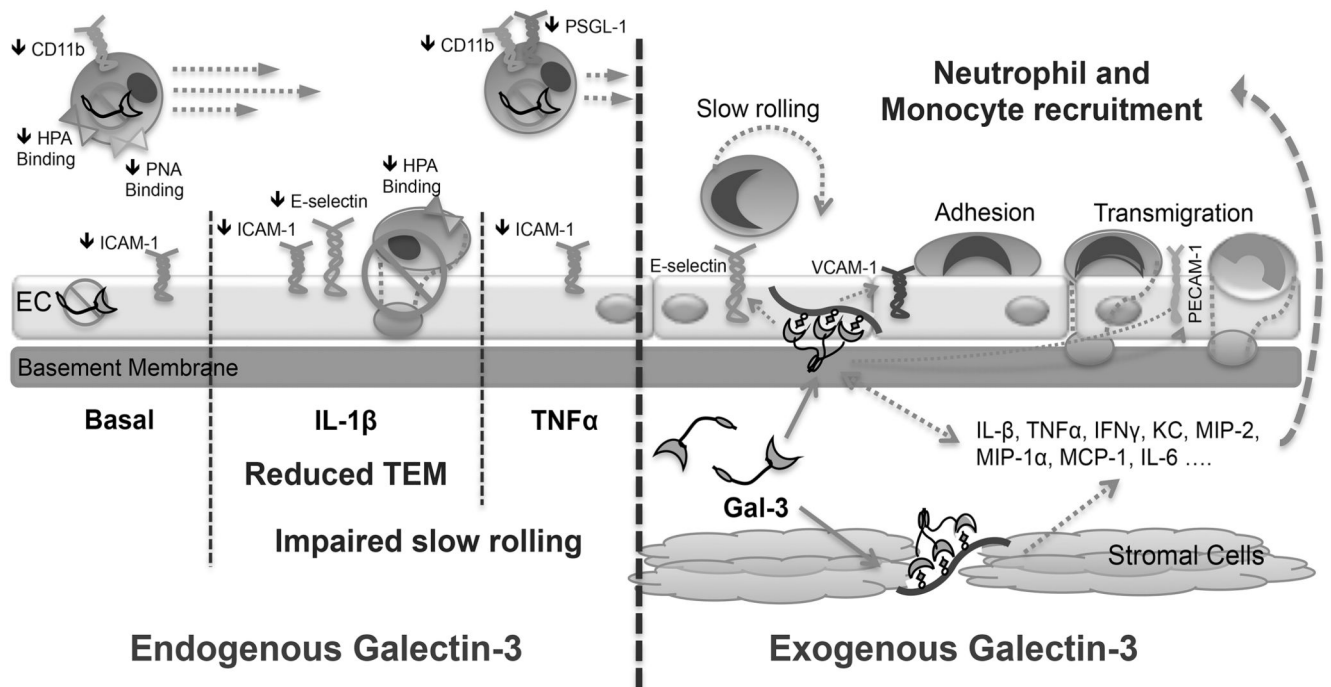
Fig. 7. Gal-3 is a positive regulator of leukocyte recruitment to the inflamed microcirculation.
In the absence of endogenous Gal-3 adhesion molecule expression is reduced on circulating neutrophils and the vascular endothelium. The glycosylation profile of circulating neutrophils is also altered with reduced expression of glycans recognised by the lectins HPA and PNA. These changes correspond with impaired slow rolling of leukocytes in response to the cytokines TNFα and IL-1β, with transendothelial migration in response to IL-1β also reduced. Conversely, administration of recombinant Gal-3 upregulates pro-inflammatory cytokines and chemokines, which results in the enhanced recruitment of neutrophils and monocytes into the tissue.